Geotechnical Aspects of Underground Construction in Soft Ground, Kusakabe, Fujita & Miyazaki (eds)

Behavior of grout column reinforced clay under lateral compression

H.J.Liao
National Taiwan University of Science and Technology, Taiwan
S.F.Su
Tung-Nan Junior College of Technology, Taiwan

ABSTRACT: Grout columns have been widely used to reinforce the soft clay inside the excavation wall where soil is subjected to lateral compression. However, by installing grout columns to the soft clay, the anisotropy of reinforced clay will become more significant than clay both in strength and stiffness. This paper will evaluate the changes in undrained shear strength and shear modulus of grout column reinforced soft clay when subjected to lateral compression through a series of true triaxial tests. Finally, the improvement effect of soil reinforced with grout columns will be correlated to the shear strength and shear modulus of clay and grout material.

1 INTRODUCTION

To improve the base stability of deep excavations in naturally deposited soft clay and to reduce the excavation induced ground movement, grout columns have been widely used to reinforce the soft clay inside the excavation wall. However, it has been recognized that due to the inherent anisotropy of in-situ soft clay, the undrained shear strength for clay inside the excavation wall (major principal stress is in horizontal direction, i.e., lateral compression) is lower than that of soil located outside the excavation wall (major principal stress is in vertical direction, i.e., vertical compression). Such a strength anisotropy nature of soft clay has certain influence on the base stability analysis of deep excavation (Hashash and Whittle, 1996 and Su et al., 1998). The degree of anisotropy will be further increased, when grout columns are installed to the soft clay either by jet grouting method or by deep mixing method. So, the mechanical behavior of grout column reinforced clay will become more sensitive to loading orientation. However, such an anisotropic effect on the undrained shear strength as well as the stiffness has seldom been discussed in the literature. So, this paper will evaluate the changes in undrained shear strength and stiffness of grout column reinforced soft clay when subjected to lateral compression (i.e., inside the excavation wall). Finally, the improvement effect of soil reinforced with grout columns will be correlated to the strength and stiffness of clay and grout.

2 TRUE TRIAXIAL APPARATUS

The true triaxial apparatus (Fig. 1) used in this study was the Colorado University type (Ko & Scott, 1967). Specimen size was cuboidal in shape and with a dimension of 100mm ×100mm ×100mm. Soil specimen was in contact with rubber membrane in six faces to separate the specimen and the pressurized water which could be used to apply loading independently in three directions to the specimen. However, due to the edge effect occurred at the edges of the rubber membranes, the load actually applied to the specimen tends to be less than the load provided by the pressurized water (Su et al., 1997). So, some correction on the measured principal stress is needed. After corrected with edge

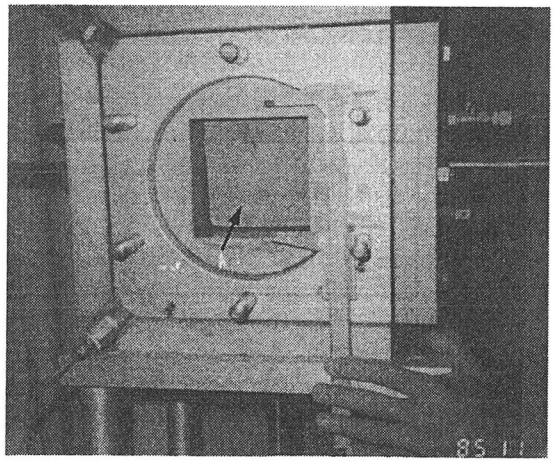

Figure 1. Schematic diagram of true triaxial device.

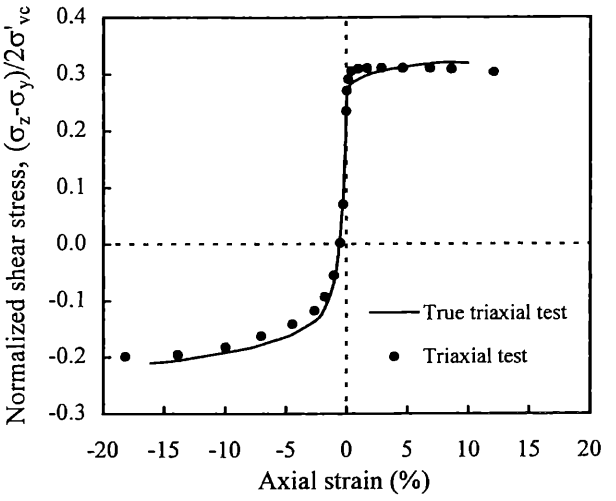

Figure 2. Comparison of true triaxial and traditional triaxial test results of Taipei silty clay (Su et al., 1997).

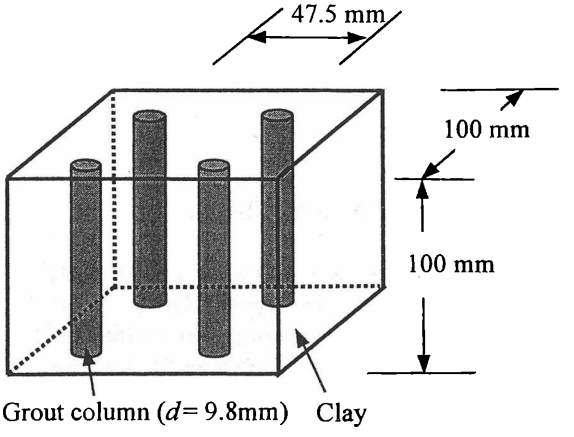

Figure 3. Specimen reinforced with 4 grout columns.

effect, the stress-strain behavior obtained from the true triaxial apparatus can be very close to that of traditional triaxial apparatus (Fig. 2). It justifies the suitability of the true triaxial apparatus on generating meaningful test data for this study.

3 SPECIMEN PREPARATION

The soil used in this study was a typical Taipei silty clay (CL). Its liquid limit was equal to 39 % and its plasticity index was equal to 15 %. Soil specimen was oven dry first and then crushed. By collecting the soil passing #40 sieve and adding water with an amount equal to 1.5 times liquid limit, a thick soil slurry used to prepare remolded soil specimen was made. Soil slurry was then poured into a Rowe-type consolidation cell and then consolidated under a pressure of 100 kPa which was applied in three stages at equal pressure. The water content of soil after consolidation was about 36%.

The grouting material of the grout column was made by mixing the remolded clay with Portland cement. The mixing proportion a_w between cement and dry clay is 3 : 10 by weight. The amount of water added was equal to the weight of cement used in the mixture, i.e., the water / cement ratio is equal to 1: 1.

Remolded soil specimen was then trimmed to a cube and placed into a mold with hole openings at top and bottom plates. A piano wire was pushed through the soil specimen from the openings on top and bottom plates. Soil was removed gradually to form a cylindrical hole with a inner diameter of 9.8 mm. By injecting the clay-cement grout to the cylindrical hole, a grout column was formed inside the soil specimen. Soil around the grout column was expected to be only slightly disturbed by the above procedure. By repeating the same procedure, specimen with 4, 9, 16 grout columns can be prepared (Fig. 3). For these three types of specimen, the center-to-center spacings between columns are equal to 47.5 mm, 31.7 mm, and 23.8 mm; the improvement ratios (I_r) are equal to 3.3%, 7.5%, and 13.3% respectively (note: the improvement ratio I_r is defined as the ratio between cross section area of grout column and unit cross section area of soil).

After the grout column developed its initial strength, the specimen was placed into the true triaxial apparatus for saturation and K_o consolidation. In general, a 5mm decrease in specimen height could be resulted after K_o consolidation. So the initial height of grout column was kept 5mm shorter than that of soil specimen to allow for the specimen height decrease after consolidation and to minimize the effect of grout columns on soil consolidation. In average, it took three days to complete the above process.

4 UNDRAINED STRESS PATH TEST

To simulate the lateral compression condition for soil inside the excavation wall, two stress paths on the octahedral plane (θ = 120° and 150°) were chosen for the stress path test (Fig. 4). Usually, θ is defined as the angle between the symmetric axis of material (i.e. z-axis or gravity direction) and stress path; while $\bar{\theta}$ is defined as the angle between major principal stress and stress path and is expressed in Eq. 1. The relationship between $\bar{\theta}$ and θ is shown in Fig. 4.

$$\tan(\bar{\theta}-\frac{\pi}{6})=\frac{1}{\sqrt{3}}\frac{2\sigma_2-\sigma_1-\sigma_3}{\sigma_1-\sigma_3} \qquad |\bar{\theta}|\le 60^\circ \qquad (1)$$

where σ_1, σ_2, and σ_3 are the major, intermediate and minor principal stresses respectively.

As shown in Fig. 4, the initial stress state ($\sigma_z = \sigma'_{vc} > \sigma_y = \sigma_x = K_o\sigma'_{vc}$, σ'_{vc} is the vertical consolidation pressure, K_o is the coefficient of lateral earth

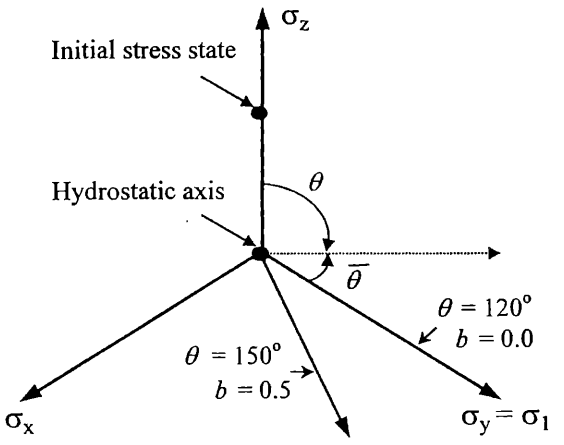

Figure 4. Stress paths on the octahedral plane.

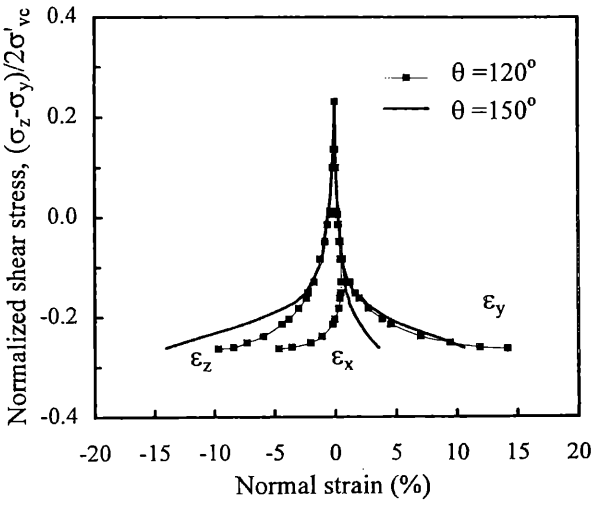

Figure 5. Comparison of stress path test results for θ =120° and θ =150°.

pressure at rest) after K_o consolidation is located above the hydrostatic axis. Then stress path movesvertically downward to the origin (the hydrostatic axis). During this stage, two lateral pressures are increased to σ_z (i.e., $\sigma_z = \sigma_y = \sigma_x = \sigma'_{vc}$). Starting from the hydrostatic axis, the direction of stress path is controlled by the principal stress ratio (b) which is defined as:

$$b = \frac{\sigma_2 - \sigma_3}{\sigma_1 - \sigma_3} \qquad (2)$$

For the stress path test θ = 150°, its major principal stress = σ_y, intermediate principal stress = σ_x, and minor principal stress = σ_z. So, the stresses applied to the specimen in three directions can be determined from Eq. 2 with b value equal to 0.5. Similarly, the principal stresses of stress path θ = 120° can be obtained with b = 0.

The true triaxial test results of remolded Taipei silty clay tested with θ = 120° and θ = 150° are shown in Fig. 5. The vertical coordinate of Fig. 5 is the normalized shear stress $(\sigma_z - \sigma_y)/2\sigma'_{vc}$, where the absolute value of $|(\sigma_z - \sigma_y)/2|$ is the largest shear stress of the three. For both the stress paths of θ = 120° and 150°, the portion of stress path between the initial stress state and the hydrostatic state (shear stress = 0) is the same (refer to Fig. 4). So the stress-strain curves in three directions are almost identical (Fig. 5). When the loading continues, the intermediate principal strain ε_2 (= ε_x) of stress path θ = 120° becomes negative (i.e., expansion); but the ε_2 (= ε_x) of stress path θ = 150° becomes positive (i.e., contraction). So, these two stress paths adopted in this study can cover the range of stress path for specimens subjected to lateral compression under plane strain condition (ε_2 = ε_x = 0).

5 TEST RESULTS

Specimens tested in this study include the clay (I_r = 0%) and the grout column reinforced clay with I_r = 3.3%, 7.5%, and 13.3%. When tested following the stress path of θ = 120°, the stress state changes from the initial K_o condition ($\sigma_z > \sigma_y$) to the lateral compression condition ($\sigma_z < \sigma_y$). The relationships between normalized shear stress $(\sigma_z - \sigma_y)/2\sigma'_{vc}$ and normal strain for various I_r are shown in Fig. 6. The higher the I_r value, the more shear resistance can be generated from the reinforced clay. For the same loading condition, the higher the I_r value, the smaller the major principal strain ε_y. So does the minor principal strain ε_z. The normalized undrained shear strengths of these three specimens determined from the CK_oU true triaxial tests are equal to 0.264 (I_r = 0%), 0.297 (I_r = 3.3%), 0.331 (I_r = 7.5%), and 0.353 (I_r = 13.3%). The normalized shear strength also increases with the I_r value.

To evaluate the strength of clay with or without grout columns reinforcement, the test results shown in Fig. 6 are replotted in Fig. 7 in terms of normalized octahedral shear stress (τ_{oct}/σ'_{vc}) and octahedral shear strain (γ_{oct}). The normalized tangential shear modulus G_t/σ'_{vc} can be determined (Fig. 8) from the curves in Fig. 7 and the following equation:

$$\frac{G_t}{\sigma'_{vc}} = \frac{d\left(\frac{\tau_{oct}}{\sigma'_{vc}}\right)}{d\gamma_{oct}} \qquad (3)$$

As shown in Fig. 8, the normalized tangential shear modulus G_t/σ'_{vc} increases with increasing improvement ratio I_r but decreases with increasing normalized shear stress $(\sigma_y - \sigma_z)/2\sigma'_{vc}$. However, specimens with the normalized shear stress $(\sigma_y - \sigma_z)/2\sigma'_{vc}$ greater than 0.15, the improvement ratio I_r

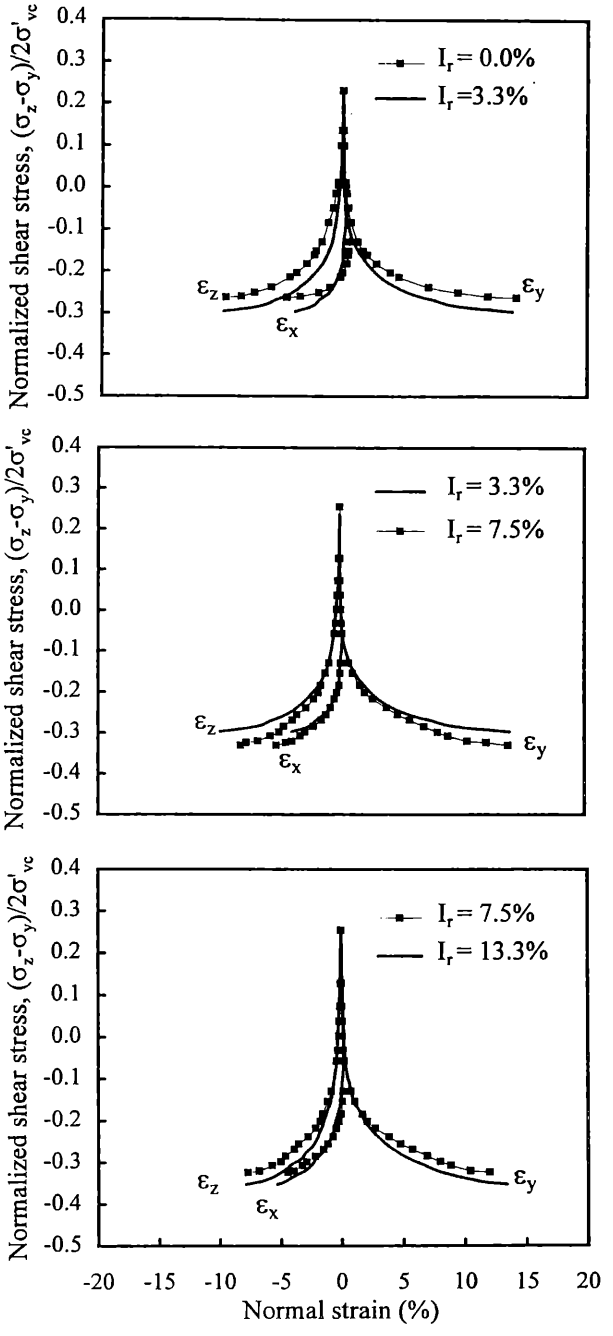

Figure 6. Comparison of stress path test results for I_r = 0.0%, 3.3%, 7.5% and 13.3% (θ = 120°).

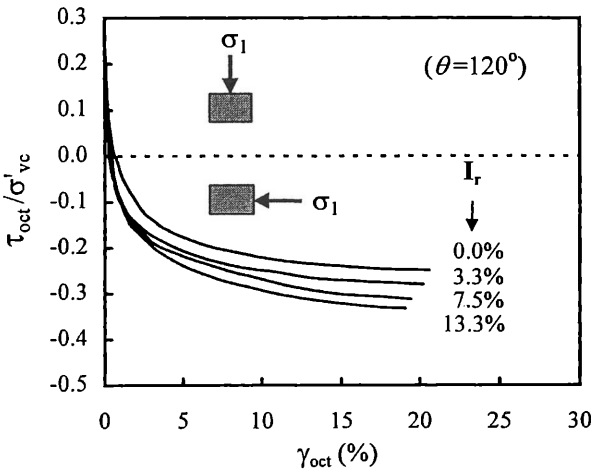

Figure 7. Normalized octahedral shear stress vs. octahedral shear strain for different improvement ratios.

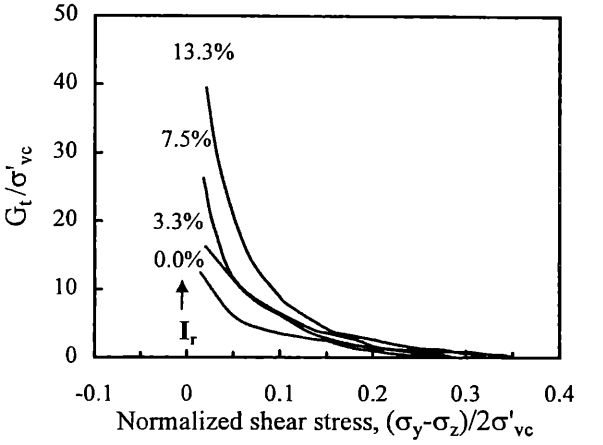

Figure 8. Normalized tangential shear modulus vs. normalized shear stress for different improvement ratios (θ =120°).

does not show much effect on the normalized tangential shear modulus G_t/σ'_{vc}. Finally, it should be noted that the portion of stress path between the initial K_o stress state and shear stress = 0 does not follow the stress path of θ = 120°. So the shear modulus of this portion is not shown in Fig. 8.

The undrained stress-strain curves for the θ = 150° stress path test are shown in Fig. 9. Similarly, the relationship between normalized octahedral shear stress (τ_{oct}/σ'_{vc}) and octahedral shear strain (γ_{oct}) and the relationship between normalized tangential shear modulus G_t/σ'_{vc} and normalized shear stress $(\sigma_z - \sigma_y)/2\sigma'_{vc}$ can be obtained from the true triaxial test results. In general, the results of stress path θ = 150° are very similar to those of stress path θ = 120°. The normalized undrained shear strength increases with the increasing improvement ratio I_r from 0.258 (I_r = 0%) to 0.290 (I_r = 3.3%), 0.342 (I_r = 7.5%), and 0.411 (I_r = 13.3%) (Fig. 10). So does the normalized shear modulus G_t/σ'_{vc} (Fig. 11).

6 EVALUATION OF IMPROVEMENT EFFECT

To evaluate the improvement effect of grout column on undrained shear strength and stiffness of clay under lateral compression, the undrained shear strength of specimens with different improvement ratios is normalized with the undrained shear strength of clay (I_r = 0%) (Fig. 12). Similarly, the normalized tangential shear moduli G_t/σ'_{vc} at normalized shear stress $(\sigma_y - \sigma_z)/2\sigma'_{vc}$ = 0.02 for different improvement ratios will be chosen to

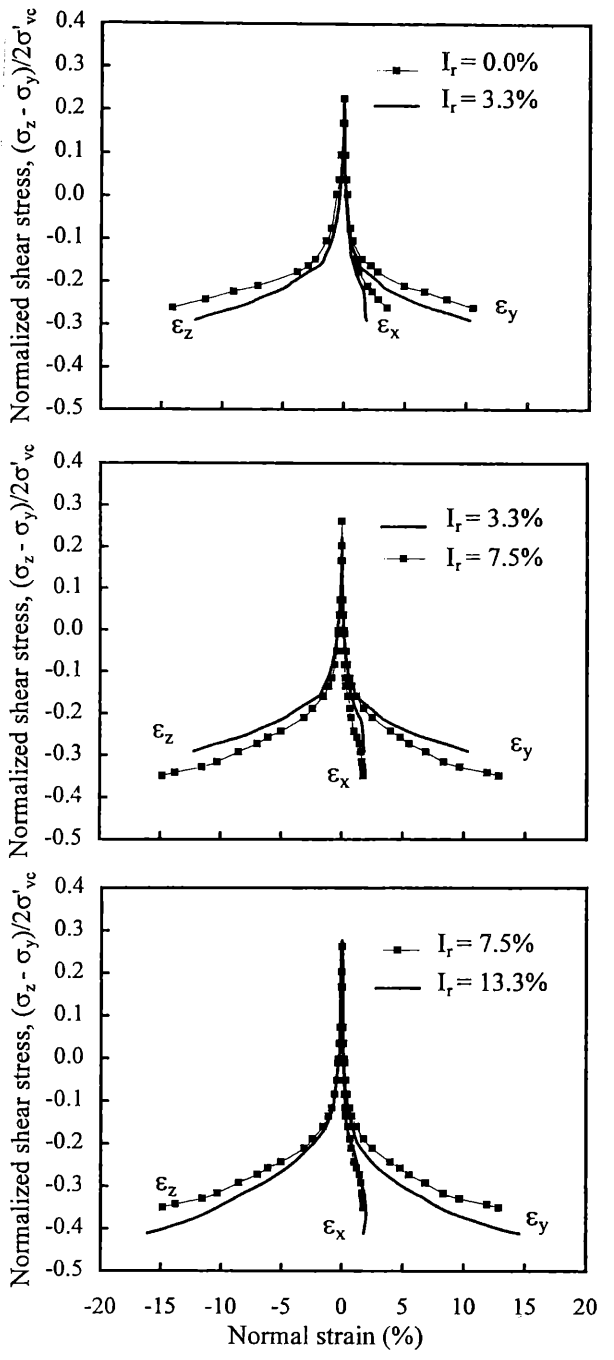

Figure 9. Comparison of stress path test results for I_r=0.0%, 3.3%, 7.5% and 13.3% (θ = 150°).

represent the G_t at small strain and normalized with that of clay. As summarized in Fig. 12, the rate of shear modulus increase with increasing improvement ratio is more significant than that of shear strength. When the improvement ratio I_r increases from 0% to 13.3%, only a 48% increase in shear strength is observed while a 290% increase in tangential shear modulus can be found. However, the effect of grout column reinforcement on increasing soil stiffness is obvious only at low stress level, say normalized shear stress $(\sigma_y - \sigma_z)/2\sigma'_{vc} < 0.15$ (refer to Figs. 8 and 11) which corresponds a normal strain less than

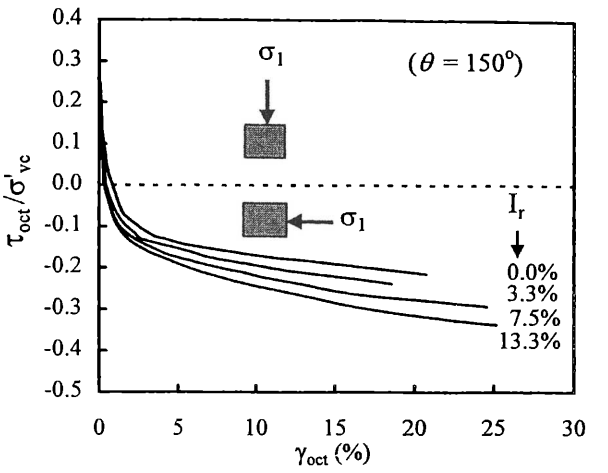

Figure 10. Normalized octahedral shear stress vs. octahedral shear strain for different improvement ratios.

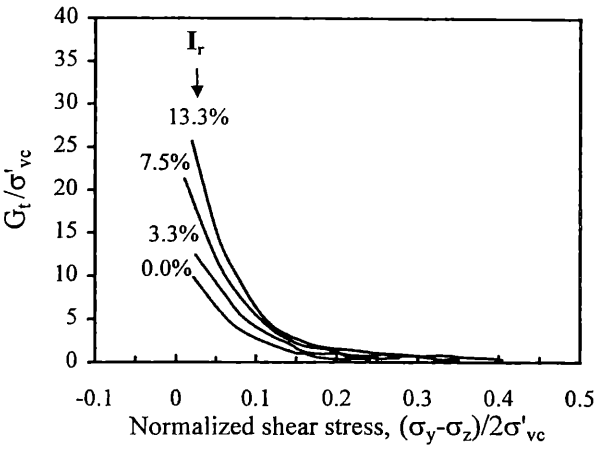

Figure 11. Normalized tangential shear modulus vs. normalized shear stress for different improvement ratios (θ =150°).

2.5%; no noticeable difference in soil stiffness compared with the clay can be observed if the stress level becomes higher. For a deflected but still stable excavation wall, the excavation induced soil deformation will not be significant. It indicates that such an increase in G_t/σ'_{vc} at small strain for grout column reinforced clay can make a great influence on controlling the lateral deflection of the excavation wall and the ground surface settlement as well.

To make the results of this study practically useful, the improvement effect of grout columns on increasing the undrained shear strength and tangential shear modulus at small strain of reinforced clay will be correlated to the undrained shear strengths and the tangential shear moduli of grout material and untreated clay obtained from the lateral compression test. So, the ratio of strength improvement (R_{si}) and the ratio of modulus improvement (R_{mi}) are defined as follows:

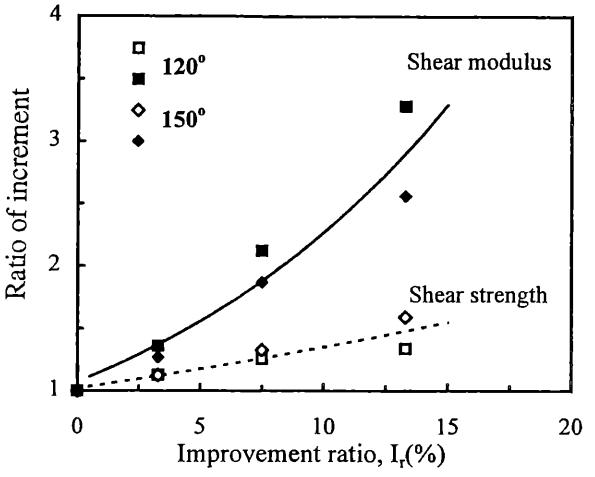

Figure 12. Ratios of increment for tangential shear modulus and shear strength at different improvement ratios (θ = 120° and 150°).

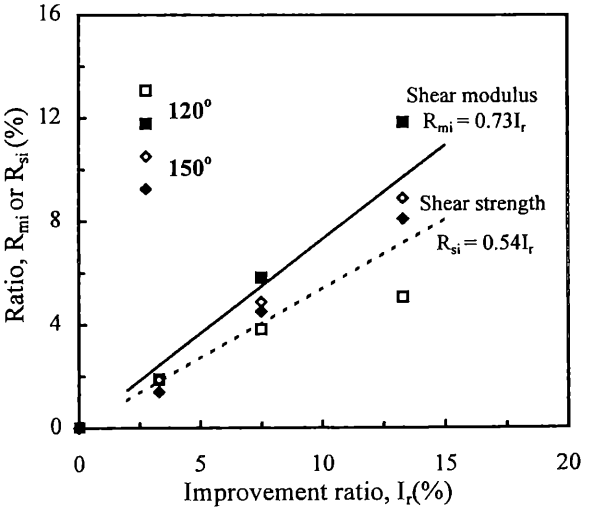

Figure 13. R_{si} and R_{mi} vs. I_r for θ =120° & 150°.

$$R_{si}(\%) = \frac{S(I_r) - S(0\%)}{S(100\%) - S(0\%)} \quad (4)$$

$$R_{mi}(\%) = \frac{M(I_r) - M(0\%)}{M(100\%) - M(0\%)} \quad (5)$$

where $S(I_r)$ and $M(I_r)$ are the normalized undrained shear strength and normalized tangential shear modulus of grout column reinforced clay with any improvement ratio I_r. S(0%) and S(100%) are the normalized undrained shear strengths of clay (I_r = 0%) and grout material (I_r = 100%). The S and M for grout material subjected to lateral compression are equal to 2.0 (= S(100%)) and 226.4 (= M(100%)) respectively (Note: grout material can be treated as isotropic material which does not much affected by the change in stress path direction); for the clay, S(0%) are equal to 0.264 (θ = 120°) and 0.258 (θ = 150°); M(0%) is equal to 12.5 (θ = 120°) and 9.85 (θ = 150°). By substituting the above parameters to Eqs. 4 and 5, the changes of R_{si} and R_{mi} with improvement ratio and stress path can be shown in Fig. 13. As a first approximation, a linear relationship is adopted to correlate R_{si} and R_{mi} with I_r:

$$R_{si} = 0.54\, I_r \quad (6)$$

$$R_{mi} = 0.73\, I_r \quad (7)$$

The above equations are good for I_r < 15%. When the improvement ratio I_r (< 15% for this study), the undrained shear strength and shear modulus under lateral compression condition are known, $S(I_r)$ and $M(I_r)$ of grout column reinforced clay can be calculated from Eqs. 4 & 6 and Eqs. 5 & 7.

7 CONCLUSIONS

A series of CK_oU lateral compression test was carried out with the true triaxial apparatus on grout column reinforced clay. It has been found that:

1. The increase in tangential shear modulus at small strain is more significant than the increase in shear strength for grout column reinforced clay. A 290% increase in tangential shear modulus is observed when the improvement ratio I_r increases from 0% to 13.3%. So, reinforcement by grout columns is an effective method to reduce the excavation induced wall movement in soft clay.
2. By knowing the shear strengths and tangential shear moduli of grout material and clay under lateral compression condition, the shear strength and tangential shear modulus at small strain for grout column reinforced clay with various improvement ratios can be determined from Eqs. 4 & 6 and Eqs. 5 & 7.

REFERENCES

Hashash, Y. M. A. & A. J. Whittle 1996. Ground movement prediction for deep excavations in soft clay. *J. Geotech. Engrg, ASCE*, 122(6): 474-486.

Ko, H. Y. & R. F. Scott 1967. A new soil testing apparatus. *Geotechnique* 17(1): 40 - 57.

Su, S. F., H. J. Liao & Y. H. Lin 1998. Base stability of deep excavation in anisotropic soft clay. *J. Geotech. and Geoenvironmental Engrg, ASCE*, 124(9): 809-819.

Su, S. F., W. W. Chen & H. J. Liao 1997. Correction for edge effect induced pressure measurement error in true triaxial test. *Proc., 7th Conf. on Current Researches in Geotech. Engrg., in Taiwan,* Vol.1, pp. 41-46.